Surface characterization and biological evaluation of spark-eroded surfaces

A. WENNERBERG*, C. HALLGREN, C. JOHANSSON, T. SAWASE
Department of Biomaterials/Handicap Research, Institute for Surgical Sciences, Medicinaregatan 8, 413 90 Göteborg, Sweden

J. LAUSMAA
Department of Materials Technology, Swedish National Testing and Research Institute, P.O. Box 857, 501 15 Borås. Sweden

Forty commercially pure titanium implants were prepared with a spark-eroding process in order to create highly increased surface roughnesses. Two degrees of roughness were achieved by altering the applied current. Surface topographical characterization was performed with SEM and an optical profilometer. The surface composition and oxide layer were investigated using Auger scanning microscopy. In the present study, there was a large difference between the stipulated and measured surface roughness, indicating the need for a careful surface characterization in each new study. After 12 wk in rabbit bone, no statistically significant difference was found with respect to peak removal torque and histomorphometric analyses. The results from the present study provide no support for further increase of the surface roughness than that possible to achieve with a blasting technique.

1. Introduction

Different aspects of surface properties, such as chemical, physical, mechanical and topographical, have gained interest from several authors as being important for implant incorporation [1–4]. Studies concerning surface topography in soft tissue have stressed that not only the degree of surface roughness but also the orientation of the structure will influence the tissue response [5, 6]. In bone tissue, the chemical treatment and composition has been found to influence implant fixation [7–9]. For blasted surfaces, experimental evidence indicates that an average height deviation of 1.5 μm is optimal for bone tissue [10–14]. Whether this value is optimal for all topographical modifications, is yet not known. The purpose of the present study was to create highly increased surface roughnesses compared with the as-machined, turned surface and with a more rounded curvature of the individual irregularities than with blasted surfaces. To achieve this goal, a spark-eroding technique was used.

2. Material and methods

2.1. Animals and anaesthesia

Ten adult, New Zealand White rabbits of both sexes were used in the present experiment. They were all aged between 10 and 12 months, with closed physes, as evinced by X-rays. Before operation, the skin of the hind limbs was shaved and washed with a mixture of iodine and ethanol, and the rabbits received an antibioticum, PenoVet® (Boeringer, Denmark) at a dose of 0.5 ml per animal.

The animals were anaesthetized with intramuscular injections of Hypnorm Vet®, (Janssen-Cilag Ltd, Saunderton, UK) at an initial dose of 0.25 ml per kg body weight and intraperitoneal injections of Apozepam® (Apothekarnes Laboratorium, Norway) at a dose of 0.25 mg per animal. If necessary, additional doses of Hypnorm were given during surgery. Locally, at the implant sites, 1.0 ml 5% Xylocain® (Astra, Sweden) was administered. An analgesic Temgesic®, (Reckitt and Colman, UK) was administered immediately after the surgery at a dose of 0.3 ml per rabbit. The animals were kept in cages, fed with a standard pellet diet and had free access to tap water. Post-operatively, the animals were supported with conventional antibiotic and analgesic therapy for 3 days. Twelve weeks after the surgery, the animals were euthanized with an overdose of Mebumal Vet®, (Nordvacc, Sweden).

2.2. Implant surface preparation and surface characterization

Forty turned commerically pure (c.p.) titanium screws with a length of 7 mm, an outer diameter of 3.7 mm,

Selected paper from the 13th European Conference on Biomaterials, Göteborg, Sweden.

a core diameter of 3.1 mm and with a pitch height of 0.6 mm, were prepared with a spark-eroding process. A conductive mask was created to fit the surface and by altering the applied current, different degrees of surface roughness were created. The manufacturer of the spark-eroding equipment, Agietron 200® (Losone-Locarno, Schweiz), supplied numerical values for the estimated average height deviation, R_a, if a certain current was used. Two current levels supposed to result in two highly increased surface roughnesses compared with the as-machined state, were chosen, $R_a = 2.7$ and 7.8 μm. An R_a (or S_a for three-dimensional measurements) value of 2.7 μm is within the possible range achievable with a blasting technique, while an R_a value of 7.8 μm is difficult to achieve for screw-shaped oral implants using other methods, for example by abrasive blasting. After the spark-eroding process, all implants were cleaned in an ultrasonic bath using trichlorethylene and rinsed twice in absolute ethanol. The spark-eroding process removes material and therefore is a comparison of the major shape between untreated and surface-modified implants needed. A Nikon Measurescope 10® (Nikon, Tokyo, Japan) equipped with a digital counter was used for this purpose.

2.3. Surface topographical characterization

One sample of each group was investigated with respect to surface topography by scanning electron microscopy (SEM, Jeol JSM-5800). Micrographs were taken at a magnification of ×500 at areas with representative topography, using a 20 keV electron beam and the secondary electron detection mode.

To control numerically the estimated R_a value created on the screw-shaped implants, an optical profilometer developed for three-dimensional measurements, TopScan 3D® (Heidelberg Instruments GmbH, Heidelberg, Germany), was used. A He–Ne laser spot, of about 1 μm diameter, was scanned across the surface of a stationary held specimen. The system uses a confocal arrangement of optics which ensures a high resolution in height, (the optical axis Z). Numerical values for different three-dimensional surface roughness parameters and visual images were produced by appropriate softwares. Wennerberg *et al.* have previously described [15] and controlled [16] the system in more detail. Three screws from implants with a presumed R_a value (S_a for three dimension) of 2.7 μm (type 1), and three from the 7.8 μm implants (type 2), chosen at random, were measured on three flanks, three thread-tops and three thread-bottoms each. The implants were then turned around and measured on the opposite side in the same manner. This makes a total of 18 measurements for each one of the six screws. The measuring area was 245 μm × 245 μm for all measurements. A larger area, depending on the strong curvature of the specimens, does not give an adequate measure. A Gaussian filter was used to exclude form and waviness from roughness. For quantitative characterization, some of the three-dimensional parameters recommended by Stout *et al.* [17], were used. The Gaussian filter size was set to 50 μm × 50 μm. The chosen three-dimensional parameters describes the surface from a vertical and a horizontal aspect.

2.3.1. Amplitude parameter, i.e. height description

S_a (R_a for two dimensions) is the arithmetic mean of the absolute values of the surface departures from a mean plane within the sampling area. The parameter is measured in micrometres and is a general and commonly used parameter.

2.3.2. Spatial parameter, space descriptive parameters

S_{cx} (S_m for two dimensions) This parameter represents the average mean spacing of profile peaks at the mean plane. According to the definition of the parameter, a peak is the highest point of the surface between an upwards and downwards crossing of the mean plane. The parameter is measured in micrometres.

2.3.3. Hybrid parameter, includes information from height as well as space

S_{dr}, the development surface area ratio, is the ratio of the developed surface area and the sampling area.

2.4. Characterization of chemical composition and thickness of the oxide layer

The surface composition of each sample was analysed by scanning Auger electron spectroscopy (Scanning Auger microprobe, Physical Electronics PHI 660, USA). Survey spectra (30–1650 eV) were recorded from two points located in the threads of each sample. A primary electron-beam energy of 5.0 keV and beam currents around 300 nA were used, with an energy analyser resolution of 0.6%. In order to minimize electron-beam damage, the primary beam was defocused to approximately 200 μm. High-resolution spectra were also acquired from the titanium peaks in order to assess the chemical state of the surface oxides, using similar electron-beam parameters as for the surveys, but an energy analyser resolution of 0.1%.

The survey spectra were evaluated using procedures described elsewhere [18] in order to obtain relative concentrations for the detected elements. This quantification procedure does not take into account depth distributions or chemically induced variations in the atomic sensitivity factors. Therefore, the stated concentrations should not be seen as absolute concentrations, but are instead given for the purpose of comparing the composition of the samples.

Depth profiles were carried out at one point on each sample, using 1.5 keV argon ions at a sputtering rate of 3.8 nm min^{-1} as calibrated for anodic TiO_2 films. In order to minimize shadowing effects, which can

lead to serious artefacts (forward sputtering and profile broadening) on rough surfaces, a focused beam (diameter <1 mm) was used on carefully selected areas. In connection with the depth-profile measurements, survey spectra were also acquired after 2.5 min sputtering time in order to obtain the relative elemental concentration at a depth of ~ 10 nm below the surface.

2.5. Surgical technique and implant insertion

In each animal, four implants were inserted, two screws of type 1 in the left proximal metaphysis of the tibia, and two screws, type 2, in the right tibial metaphysis. All comparisons were made only between the left and right legs in the same animal. The tibial implants were incorporated 5 mm apart, and two threads were left visible above the bone surface. A controlled surgical technique was used, including careful drilling with a low rotatory speed and a profuse saline cooling. Immediately after surgery, all rabbits were allowed full weight bearing.

2.6. Torque measurements and preparation of specimens

The torque necessary to loosen the implants localized most distally in the left and the right tibia ($n = 20$) was measured with a Tohnichi 6 BTG-N® (Tohnici MFG, Japan) with a measuring range from 0–74 N cm. A slowly increasing torque was gradually applied to each implant until loosening. The tibial implants that were localized most proximally ($n = 20$), were removed *en bloc* and prepared for histomorphometrical evaluation. These implants with the surrounding tissue were fixed in 4% neutral buffered formaldehyde, dehydrated in ethanol and embedded in light-curing resin, Technovit 7200 VLC (Kultzer & Co, Germany). The cutting and grinding were performed in an Exakt sawing machine and grinding equipment as described by Donath [19]. The approximately 10 μm thick sections were stained with toluidine blue. The histomorphometric analysis was performed in a Leitz Aristoplan light microscope, equipped with a Leitz Microvid unit connected to a PC computer, enabling the observer to perform histomorphometrical quantifications directly in the eye-piece of the microscope. A $\times 10$ magnification objective and an eye piece of $\times 10$ magnification was used for all measurements. Measurements of percentage bone-to-metal contact around all threads, as well as the best three consecutive threads in the cortical region were calculated. In a similar way the amount or bone in the thread area was calculated.

2.7. Statistics

Wilcoxon signed rank test was used to calculate *p*-values for torque measurements and for the histomorphometric analysis. Each animal served as its own control.

3. Results

3.1. Shape and topographical characterization

The major shape of the implants was somewhat diminished by spark eroding with the lower current intensity, type 1, while type 2 demonstrated a very small decrease in the outer diameter and even a slightly increased core diameter (Table I).

Representative SEM images of the two surfaces are shown in Fig. 1a and 1b. There was a similar

TABLE I The outer and core diameters of c.p. titanium screws before and after surface modification with a spark-eroding process. Mean value calculated on measurements from three screws for each surface modification

	Outer diameter (mm)	Core diameter (mm)
Spark eroded type 1		
Mean value		
Screw 1–3	3.639	3.071
S.D.	0.001	0.01
Spark eroded type 2		
Mean value		
Screw 1–3	3.687	3.136
S.D.	0.009	0.004
Before surface modification		
Mean value		
Screw 1–3	3.705	3.081
S.D.	0.008	0.008

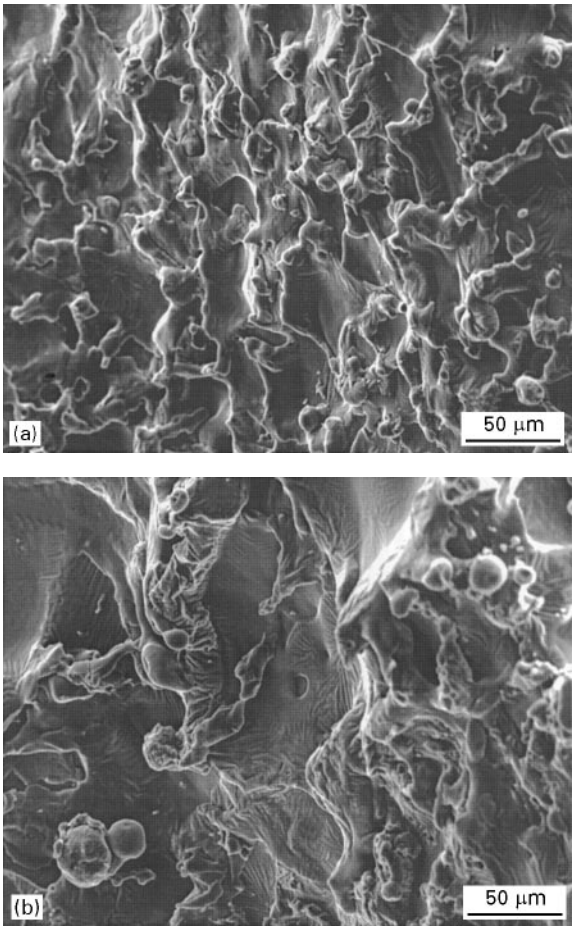

Figure 1 SEM images of spark-eroded surfaces: (a) type 1, (b) type 2.

topography all over the treated implant surfaces. The two types of implants had, qualitatively, similar topographies. On the ~ 10 μm scale, two types of area can be distinguished, one which is rough and one that is relatively smooth. The rough area consisted of irregularly shaped structures with rounded curvatures. Droplet shaped or nearly spherical structures and a few cracks could also be observed in these areas. The smooth type of areas, on the other hand, looked relatively flat with corrugations on the ~ 1 μm scale as the main features. The corrugations appeared predominantly on the borders to the rough areas. On a submicrometre scale, both type of area had a relatively smooth topography. The qualitative appearance of the surfaces thus indicated that they had undergone surface melting, as expected from the spark-eroding process. The two types of implant differed somewhat in the typical sizes of the two types of areas, which were larger on the type 2 sample. The numerical characterization of the surface roughness, as evinced by measurement with the TopScan three-dimensional equipment, demonstrated two different surface structures for the two spark-eroded surfaces, types 1 and 2 (Fig. 2a, b) evinced by the amplitude, the spatial and the hybride parameters used in the present study, even though the difference in calculated S_a value between the two modified surfaces was much smaller than the expected ones, especially for the rougher surface (type 2). The theoretically calculated R_a value for type 1 was 2.7 μm, compared to a real S_a value of 2.5 μm and for type 2, which a theoretical R_a value of 7.8 μm, the measured S_a value was 2.7 μm (Table II). The average distance between the surface irregularities in the horizontal direction was for types 1 and 2, 15.6 and 15.8 μm, respectively. The increased surface area ratio was 1.9 for type 1, and 2 for type 2.

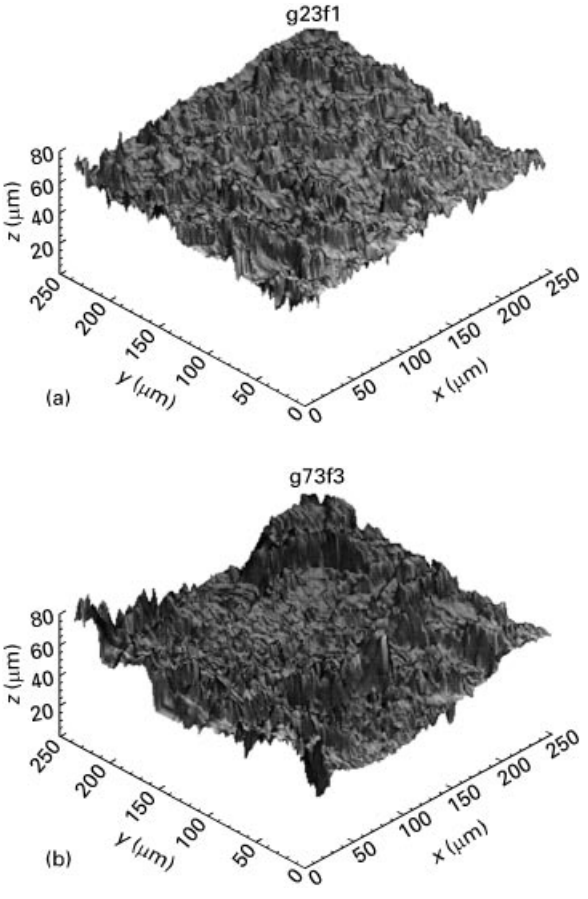

Figure 2 Computer-generated images of the two spark-eroded surfaces investigated in the present study: (a) type 1, (b) type 2.

3.2. Chemical composition and thickness of the oxide layer

Table III shows the relative concentrations of the elements detected in the AES survey analyses. All survey spectra showed clear titanium, oxygen and carbon signals. Carbon was the dominant element, with relative concentrations of 70–80 at %. The titanium levels are similar for the two samples, while the oxygen levels are significantly lower for the type 2 sample. In addition to titanium, oxygen and carbon, minor amounts (<1 at %) of calcium, chlorine, phosphorus and sulfur were also detected in some of the analysed areas. After sputtering to a depth of ~ 10 nm, the signals from the latter elements disappeared , and the oxygen signal decreased by a factor of 3–4. However, only a minor decrease in the carbon levels was observed even at this depth below the surface. The shape of the carbon signal (Fig. 3b) at this depth is, for both samples, typical for that of carbides, while at the surface (Fig. 3a) it indicates hydrocarbon or graphitic type of carbon.

High-resolution spectra of the two main titanium peaks are shown in Fig. 4. The shape of the Ti(LMV) signal at ~ 420 eV for the type 1 sample (Fig. 4a) is consistent with a TiO_2-like oxide [2, 21, 22]. For the type 2 sample (Fig. 4b) both the Ti(LMM) and Ti(LMV) peak shapes have clear shoulders on the

TABLE II Quantitative surface roughness characterization using one height, one space and one hybrid parameter

	S_a (μm)	S_{cx} (μm)	S_{dr}
Type 1 (2.7 μm)			
Screw 1	2.51	15.90	1.92
Screw 2	2.44	15.28	1.93
Screw 3	2.49	15.63	1.94
Mean 1–3	**2.48**	**15.60**	**1.93**
Type 2 (7.8 μm)			
Screw 1	2.80	16.36	2.00
Screw 2	2.62	15.32	1.93
Screw 3	2.72	15.66	1.99
Mean 1–3	**2.71**	**15.78**	**1.97**

TABLE III Relative concentrations (%) for elements detected in AES analyses

Sample (analysis point)	Ti	O	C	Ca	Cl	P	S
Type 1, surface (1)	5.7	20.0	74.1	0.0	0.1	0.0	0.1
(2)	6.0	22.9	70.7	0.0	0.2	0.0	0.2
ion-etched 10 nm	30.3	4.9	64.8	0.0	0.0	0.0	0.0
Type 2, surface (1)	5.8	15.7	77.0	0.8	0.3	0.2	0.1
(2)	5.9	11.9	81.5	0.6	0.2	0.0	0.0
ion-etched 10 nm	28.1	3.6	68.3	0.0	0.0	0.0	0.0

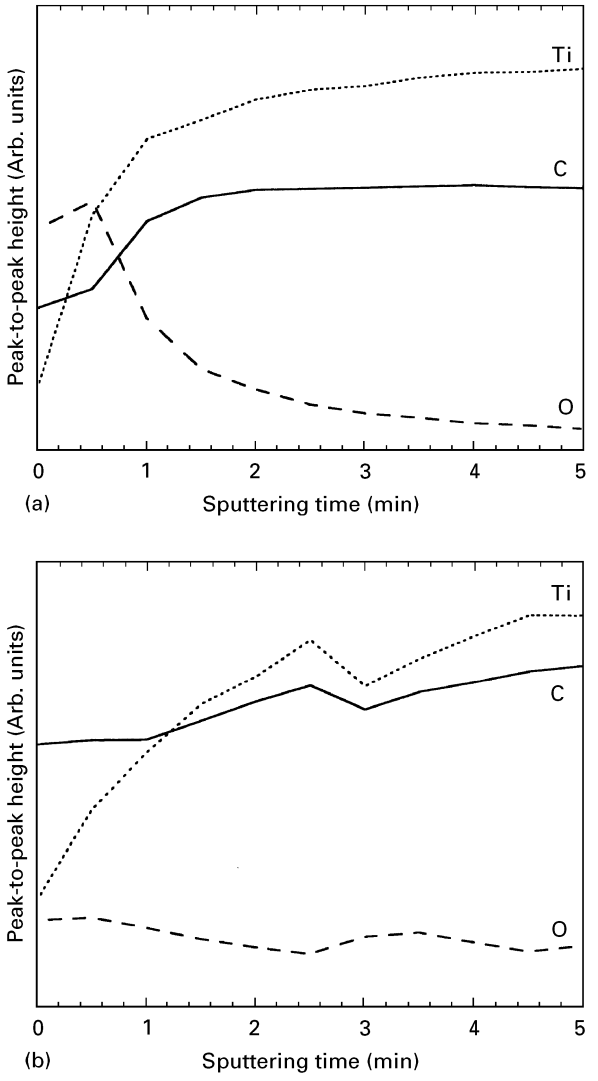

Figure 3 Line shapes of the carbon Auger peak from (a) the as received surface, and (b) after sputtering to a depth of ≈ 10 nm.

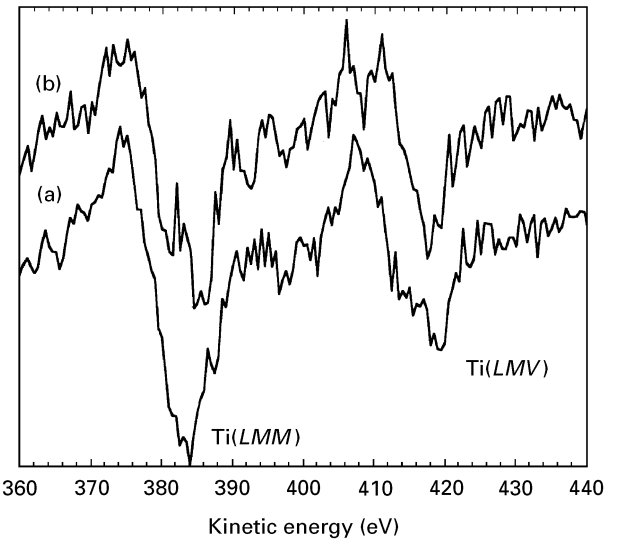

Figure 4 Line shapes of the two main titanium Auger peaks from (a) a type 1 sample, and (b) a type 2 sample.

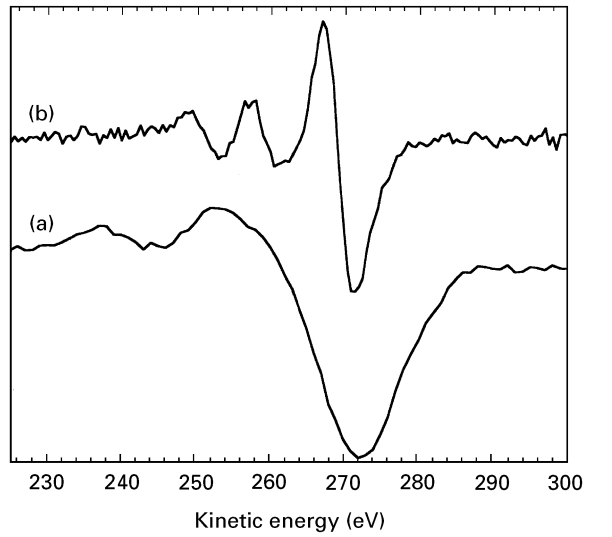

Figure 5 Depth profiles for titanium, oxygen and carbon from (a) a type 1 sample, and (b) a type 2 sample.

low-energy side, which indicates a reduced state or a thinner surface oxide.

The depth profiles from the two samples are significantly different (Fig. 5), For the type 1 sample (Fig. 5a) the titanium signal increases with depth to a nearly stable value which is reached after ~ 3 min sputtering. The oxygen signal shows a slight initial increase with depth, followed by a continuous decrease in towards the material, which is indicative of a surface oxide. Taking the depth at which the oxygen signal has decreased to half its maximum value (~ 1 min), an oxide thickness of ~ 4 nm is obtained for this sample. The carbon signal, however, increases with depth from the surface and reaches a stable value after about 2 min sputtering. For the type 2 sample (Fig. 5b), the titanium and carbon depth profiles are qualitively similar, as for the other sample. However, the oxygen signal shows a considerably lower level and a shallower decrease with depth. Owing to the shape of the oxygen profile, it is not meaningful to estimate a surface oxide thickness for this sample. Instead, the oxygen seems to be present in this sample as dissolved species with a negative concentration gradient in towards the material. For both samples, the carbon signal in the depth profiles thus gives evidence for the presence of a carbide layer below the surface oxide, in agreement with the carbon peak shapes observed in survey spectra measured after ion etching 10 nm into the material. The ultimate thickness of this carbide layer was not measured, but judging from the depth profiles, it persists to several tens of nanometres into the material.

3.3. Torque measurements

The torque necessary to loosen the implants was similar for the two types of surface modifications. The mean value was 37 N cm for type 1, and 40 N cm for type 2 (Table IV).

3.4. Histomorphometric evaluation

The histomorphometric analysis showed no statistically significant difference when the bone-to-metal

TABLE IV Removal torques of spark-eroaded c.p. titanium screws. Measurement after 12 weeks in the rabbit bone

Rabbit	Removal torque (N cm)	
	Left tibia type 1	Right tibia type 2
1	46	36
2	35	38
3	36	33
4	31	36
5	36	56
6	37	54
7	31	35
8	59	28
9	31	48
10	30	36
Mean value	37	40
S.D.	9.0	9.4

p-value calculated with Wilcoxon Signed Rank test; p-value = 0.154.

TABLE V Mean value of measured per cent bone-to-implant contact of 10 c.p. titanium implants of each surface modification. Calculations were made for the best three consecutive threads representing the situation in the cortical region and for all threads around the threaded implant

	Bone-to-implant contact (%)	
	Left tibia type 1	Right tibia type 2
All threads around the screw	13	16
(min–max value)	(23–26)	(9–23)
Best three consecutive threads	25	24
(min–max value)	(11–45)	(16–28)

p-value calculated with Wilcoxon signed rank test. p-value all threads $p = 0.121$. p-value three consecutive best threads $p = 0.439$.

TABLE VI The average amount of bone in the thread area of c.p. titanium implants. Calculations were made for the best three consecutive threads and for all thread areas around the screw. The values are based on 10 screws from each of the two surface modifications

	Average amount of bone (%)	
	Left tibia type 1	Right tibia type 2
All threads around the screw	42	45
(min–max value)	(28–57)	(35–57)
Best three consecutive threads	70	64
(min–max value)	(57–85)	(55–73)

p-value calculated with Wilcoxon signed rank test. p-value all threads $p = 0.222$. p-value three consecutive best threads $p = 0.121$.

contact was measured, nor was there any difference in the percentage of bone in the threads. When measuring the percentage bone-to-metal contact around all threads, the mean value was 13% for type 1 and 16% for type 2, and 25% for type 1, and 24% for type 2 when measuring the consecutive best three threads (Table V). The percentage of bone in all threads around the implant was 42% for type 1, and 45% for type 2. The percentage of bone in the consecutive three best threads was 70% for type 1 and 64% for type 2 (Table VI).

4. Discussion

The increased core diameter for type 2 may be explained by the higher current level producing higher walls of melted metal. The surface characterization shows that the two types of spark-erosion processes resulted in relatively similar surface characteristics. Both types of surface have a qualitatively similar surface topography, reflecting the surface melting and solidification which occurs during the surface treatment. There are some quantitative differences in the size of the structural features and in surface roughness between the two sample types. The main difference in surface composition is the lower amount of oxygen for the type 2 sample.

Both samples have a sub-surface carbide layer which seems to extend several tens of nanometres into the material. The carbide layer is presumably explained by the fact that the spark-eroding process occurs in a refined petroleum bath, where the refined petroleum works as a cooling liquid. Carbide phases in the surface are normally not observed, unless intensionally produced by, for example, chemical vapour deposition processes. Unintentional carbides can, however, be formed during glow-discharge plasma treatment if inappropriate process parameters are used [20]. Machined or polished titanium surfaces have much smoother and regular surface topographies than the present ones, and are normally covered by TiO_2-like surface oxides [2, 21]. Grit-blasted surfaces can be prepared to have similar roughnesses to that shown by the present ones, but often show a sharper surface topography and impurities, owing to the shape and composition of the blasting medium particles [14].

The small increase in surface roughness for type 2 compared with type 1, did not result in a firmer bone fixation. One reason may be that the two different surface roughnesses were too similar, On the other hand, other studies with the same magnitude of difference between the S_a value for investigated surfaces have demonstrated a statistically significant difference in removal torque and bone-to-metal contact [14, 23]. Another reason is that the optimal increase of surface roughness has already passed and no further improvement will occur. Previous studies [11, 13] give some support for this theory.

In previous work, minor changes in bone response have been observed around modified titanium surfaces with different oxide thicknesses and submicrometre topography [24, 25]. In the present study, the differences with respect to surface oxide composition and thickness were not reflected in the biological response. This study points to the fact that surface structure may not always be predictable. In this case, the manufacturer had treated flat samples and measured them with a two-dimensional technique. The measuring technique, and even more importantly, the

change from a flat sample to a screw design may explain the difference between the stipulated and actually measured surface roughnesses. A flat surface is much more easy to modify and SEM images of the spark-eroded screws demonstrated some areas with an uneven surface modification, the reason probably being a lack of a precisely fitting mask. This may be improved. However, the results from this study give no support for further increases of the surface roughness beyond that which is possible to achieve with a blasting technique.

Acknowledgements

This study was supported by grants from Sylvans' foundation, Nutek project 9305121-2 the Swedish Dental Society, the Anna Ahrenberg Foundation, the Greta and Einar Asker Foundation, the Wilhelm and Martina Lundgren Science Foundation, the Swedish Medical Research Council and the Hjalmar Svensson research foundation. The authors thank Torgny Wilmarsson for the preparation of all the spark-eroded surfaces.

References

1. B. KASEMO and J. LAUSMAA, in "The Bone-Biomaterials Interface" edited by J. E. Davis (University of Toronto Press, Toronto, 1991) p. 19.
2. J. LAUSMAA, *J. Electron Spectrosc. Rel. Phenom.* **81** (1996) 343.
3. R. E. BAIER, A. E. MEYER, J. R. NATIELLA, R. R. NATIELLA and J. M. CARTER, *J. Biomed. Mater. Res.* **18** (1984) 337.
4. K. GOTFREDSEN, A. WENNERBERG, C. JOHANSSON, L. TEIL SKOVGAARD and E. HJØRTING-HANSEN, *ibid.* **29** (1995) 1223.
5. B. CHEHROUDI, T. R. L. GOULD and D. M. BRUNETTE, *ibid.* **24** (1990) 1203.
6. *Idem*, *ibid.* **25** (1991) 387.
7. H-J. WILKE, L. CLAES and S. STEINEMANN, in "Clinical Implant Materials. Advances in Biomaterials" edited by S. Heimke, U. Soltész and A. J. C. Lee (Elsevier Science, Amsterdam, 1990) p. 309.
8. J. E. ELLINGSEN, *J. Mater. Sci. Mater. in Med.* **6** (1995) 749.
9. D. L. COCHRAN, P. V. NUMMIKOSKI, F. L. HIGGINBOTTOM, J. S. HERMANN, S. R. MAKINS and D. BUSER, *Clin. Oral Impl. Res.* **7** (1996) 240.
10. A. WENNERBERG, T. ALBREKTSSON, B. ANDERSSON and J. J. KROL, *ibid.* **6** (1995) 24.
11. A. WENNERBERG, T. ALBREKTSSON and B. ANDERSSON, *J. Mater. Sci. Mater. Med.* **6** (1995) 302.
12. A. WENNERBERG, T. ALBREKTSSON, C. JOHANSSON and B. ANDERSSON, *Biomaterials* **17** (1996) 15.
13. A. WENNERBERG, T. ALBREKTSSON and B. ANDERSSON, *J. Oral Maxillofac. Impl.* **11** (1996) 38.
14. A. WENNERBERG, T. ALBREKTSSON and J. LAUSMAA, *J. Biomed. Mater. Res.* **30** (1996) 251.
15. A. WENNERBERG, T. ALBREKTSSON, H. ULRICH and J. KROL, *J. Biomed. Eng.* **14** (1992) 412.
16. A. WENNERBERG, R. OHLSSON, B-G. ROSÉN and B. ANDERSSON, *Med. Eng. Phys.* **18** (1996) 548
17. K. J. STOUT, E. J. DAVIS, P. J. SULLIVAN, W. P. DONG, E. MAINSAH, N. LUO, T. MATHIA and H. ZAHOUANI, The development of methods for the characterization of roughness in three dimensions, EUR 15178 in "EN of commission of the European Communities" (University of Birmingham, Birmingham, 1993).
18. L. E. DAVIS, N. C. MACDONALD, P. W. PALMBERG, G. E. RIACH and R. E. WEBER, "Handbook of Auger electron spectroscopy" (Physical Electronics, Eden Prairie, 1978).
19. K. DONATH, *Der Präparator* **34** (1988) 197.
20. B-O. ARONSSON, J. LAUSMAA and B. KASEMO, *J. Biomed. Mater. Res.* **35** (1997) 49.
21. J. LAUSMAA, H. MATTSSON and B. KASEMO, *Appl. Surf. Sci.* **44** (1990) 133.
22. G. D. DAVIS, M. NATAN and K. A. ANDERSSON, *ibid.* **15** (1983) 321.
23. A. WENNERBERG, A. EKTASSABI, B. ANDERSSON and T. ALBREKTSSON, *Int. J. Oral Maxillofac. Impl.* (1997), in press.
24. C. LARSSON, P. THOMSEN, M. RODAHL, B. O. ARONSSON, J. LAUSMAA, B. KASEMO and L. E. ERICSSON, *Biomaterials* **17** (1996) 605.
25. *Idem*, *ibid.* (1997), submitted.

Received 5 May
and accepted 12 May 1997